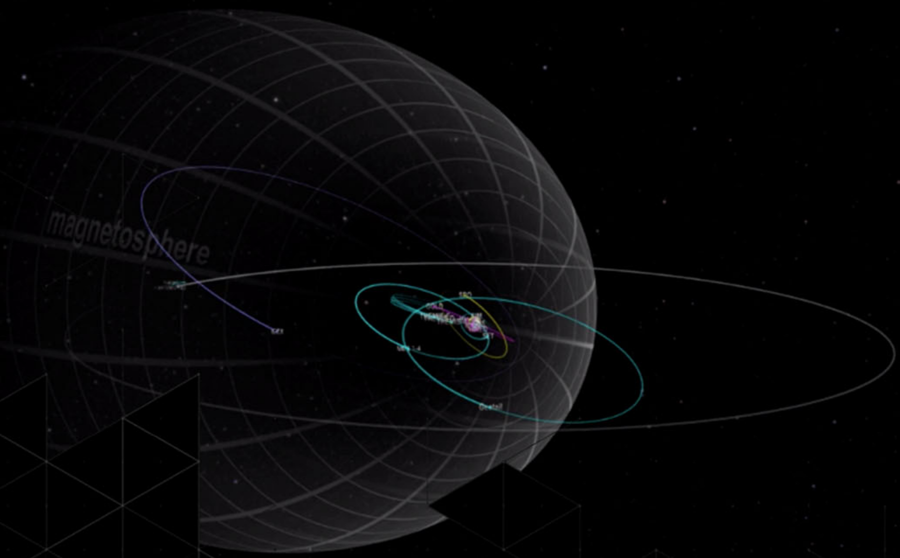

JOHNS HOPKINS
APPLIED PHYSICS LABORATORY

Multi-Point Observations

Sarah K. Vines

Magnetosphere Online Seminar Series
November 16, 2020

Multi-point observations take many forms

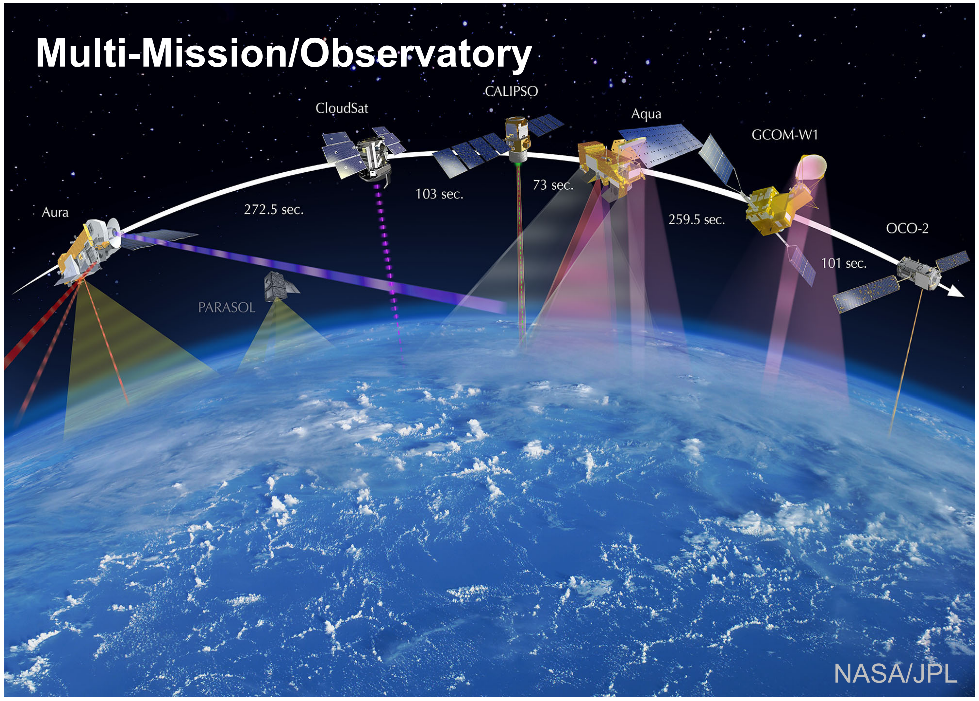

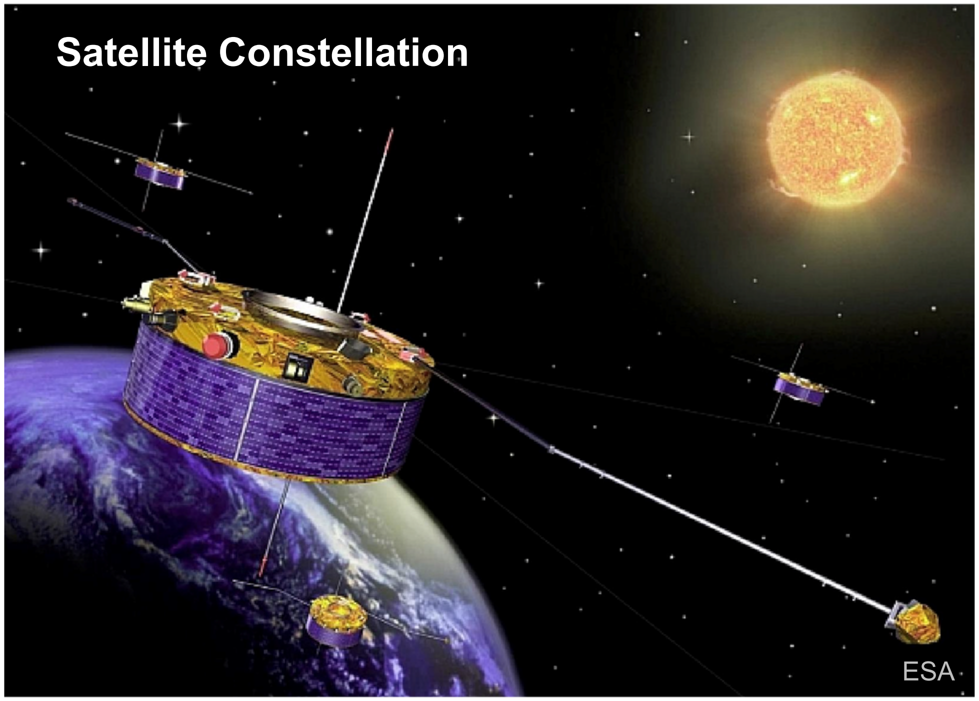

With multi-point measurements and techniques, we can explore system-wide dynamics and local variations beyond what can be done with just one observatory.

Multi-Point Observations: The Multi-Observatory View

Timing & Causality

Spatial Distribution

Measurement Synthesis

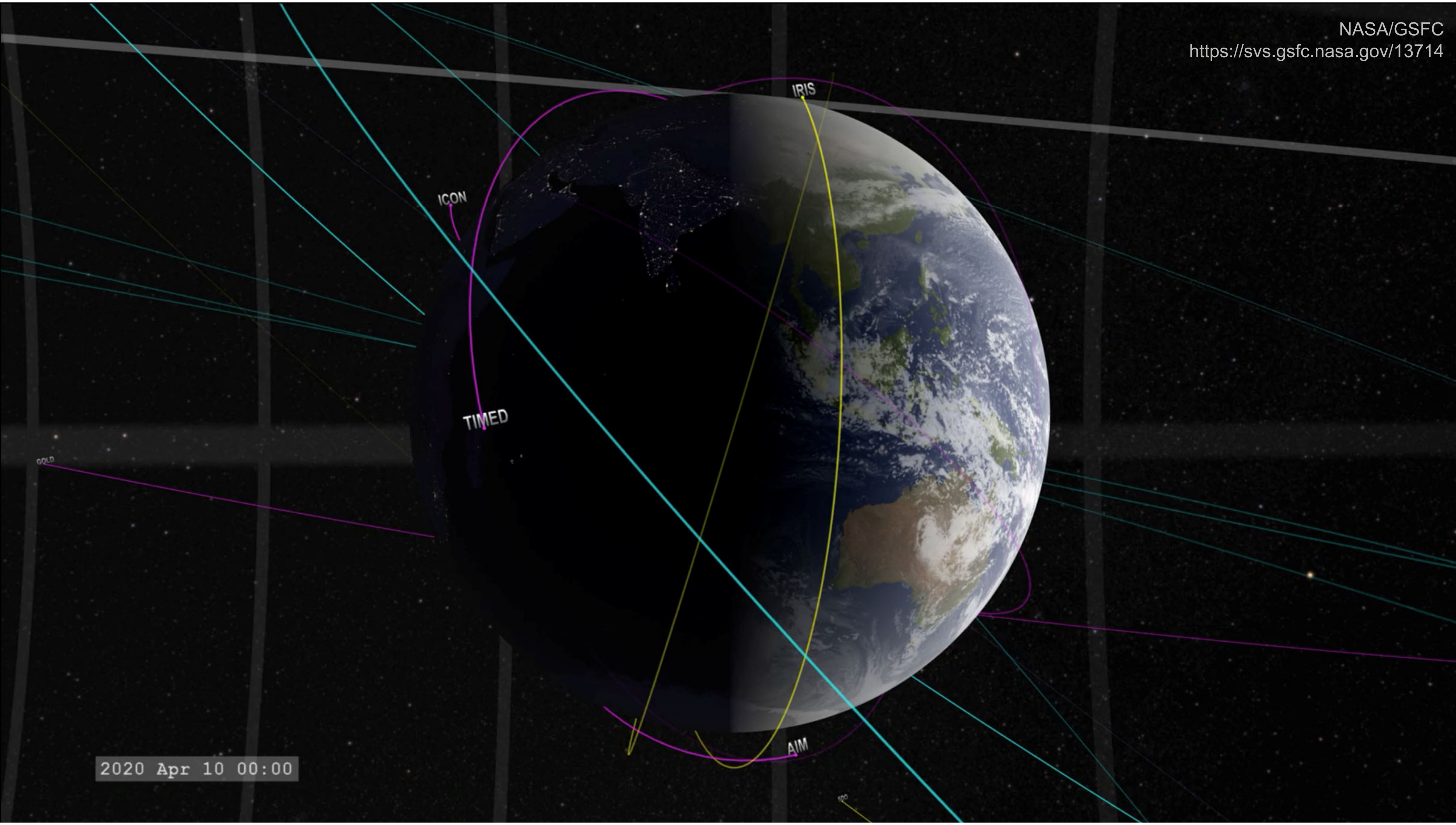
NASA/GSFC
https://svs.gsfc.nasa.gov/13714
IRIS
ICON
TIMED
AIM
2020 Apr 10 00:00

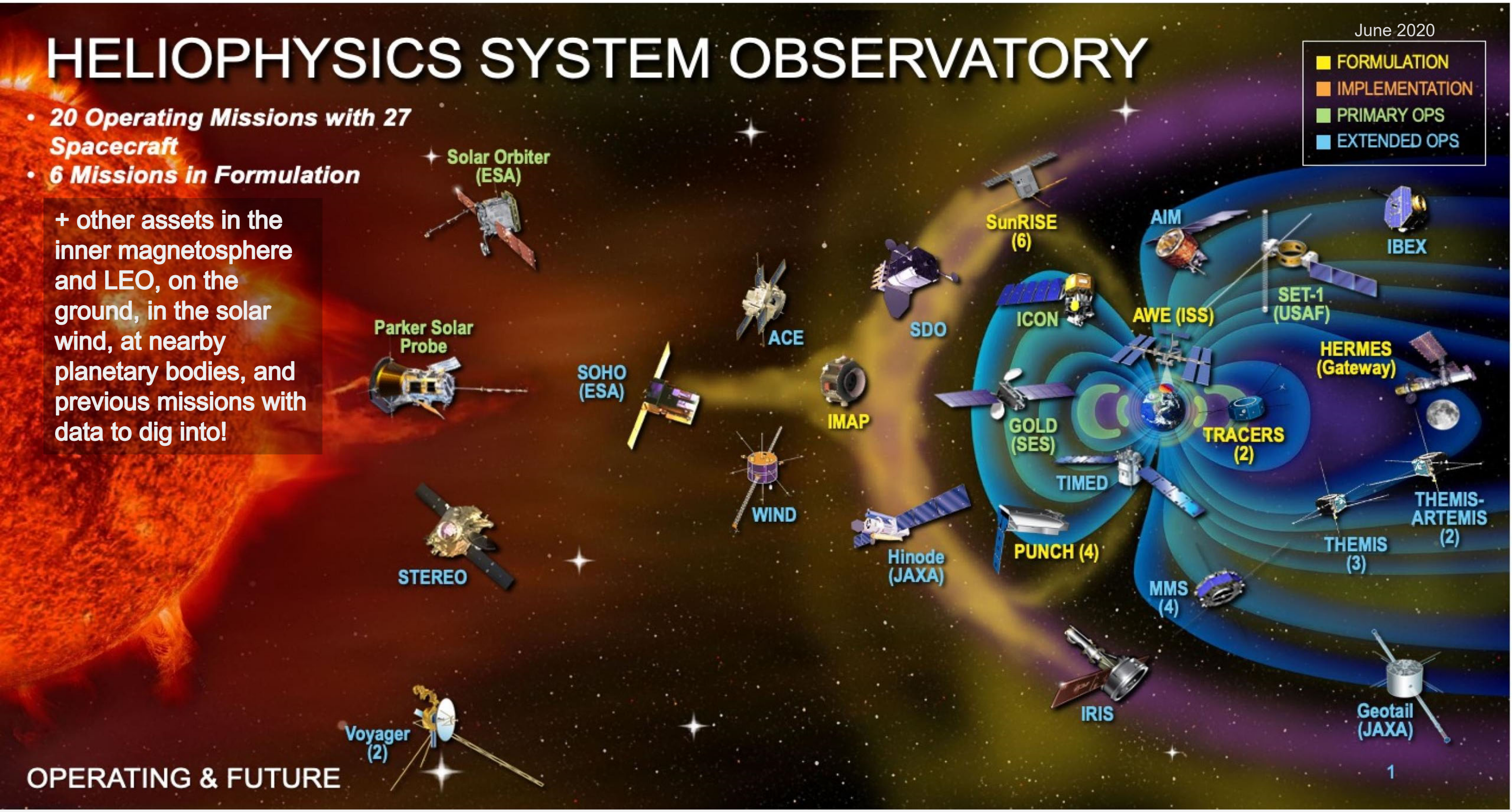
HELIOPHYSICS SYSTEM OBSERVATORY
June 2020
FORMULATION
IMPLEMENTATION
PRIMARY OPS
EXTENDED OPS
• 20 Operating Missions with 27 Spacecraft
• 6 Missions in Formulation
+ other assets in the inner magnetosphere and LEO, on the ground, in the solar wind, at nearby planetary bodies, and previous missions with data to dig into!
Solar Orbiter (ESA)
Parker Solar Probe
SOHO (ESA)
ACE
SDO
SunRISE (6)
AIM
IBEX
ICON
AWE (ISS)
SET-1 (USAF)
HERMES (Gateway)
IMAP
GOLD (SES)
TRACERS (2)
WIND
TIMED
THEMIS-ARTEMIS (2)
THEMIS (3)
STEREO
Hinode (JAXA)
PUNCH (4)
MMS (4)
IRIS
Geotail (JAXA)
Voyager (2)
OPERATING & FUTURE
1

Examples of the extended HSO at work

Timing, causality, and large-scale spatial distribution: Substorms

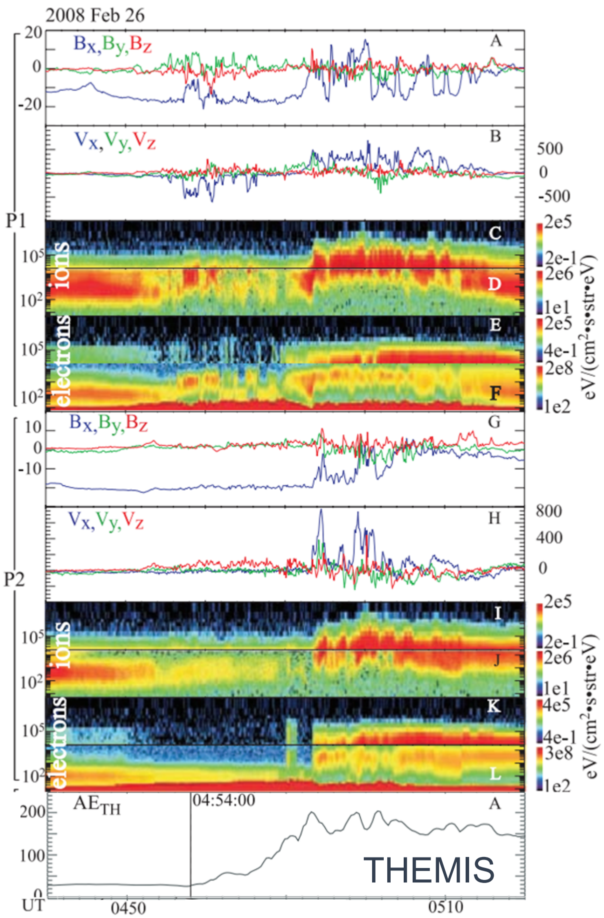

Angelopoulos et al., 2008

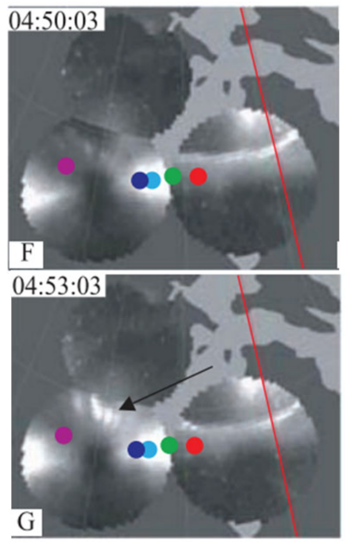

THEMIS - ASI

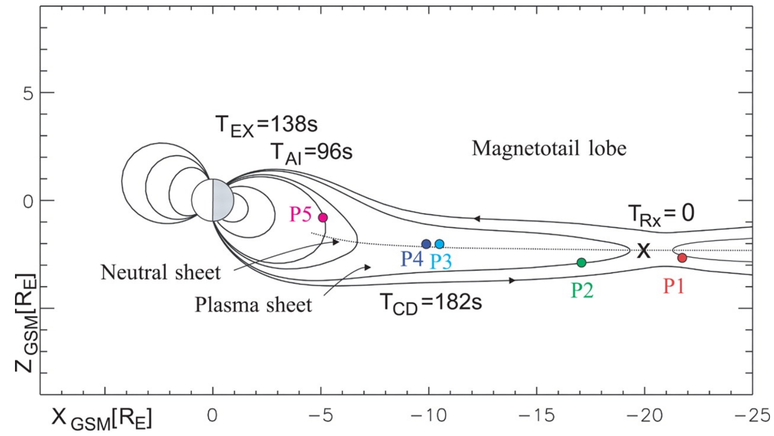

Runov et al., 2011

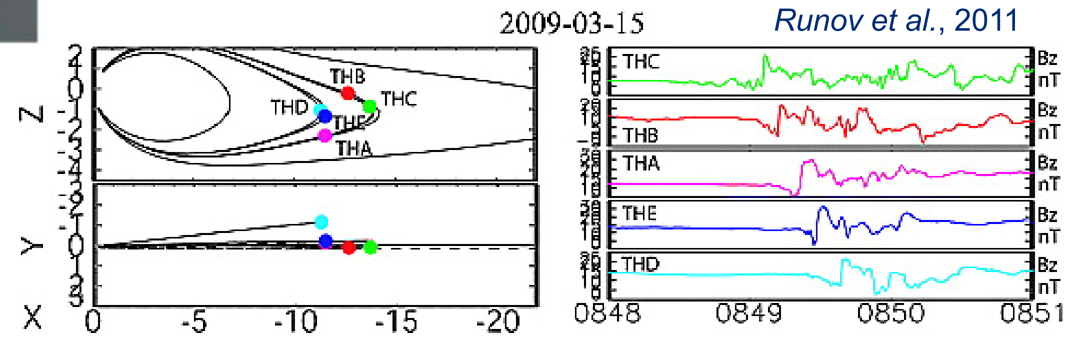

Examples of the extended HSO at work

Timing, causality, and large-scale spatial distribution: Energetic Particle Injections

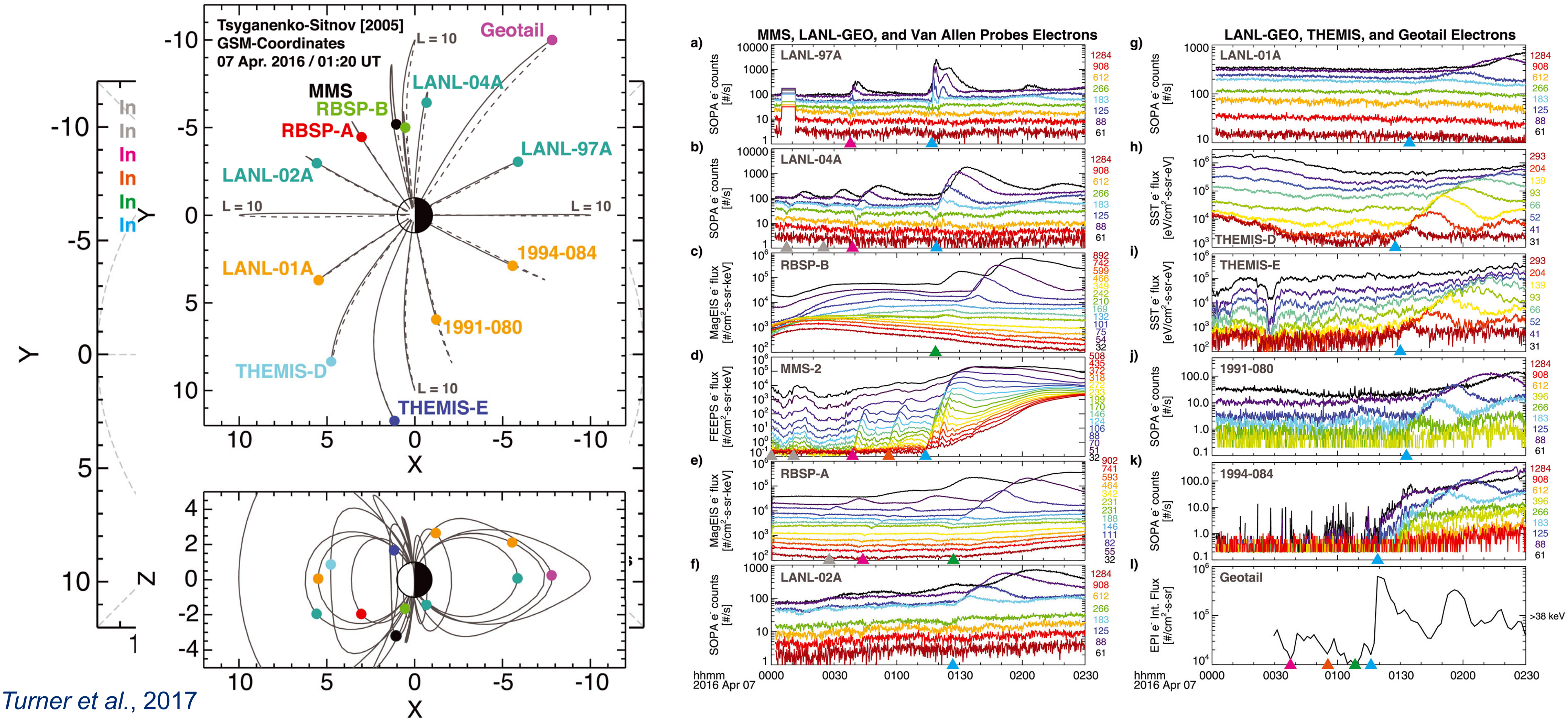

Turner et al., 2017

Examples of the extended HSO at work

Timing, causality, and large-scale spatial distribution: Wave generation

Engebretson et al., 2018

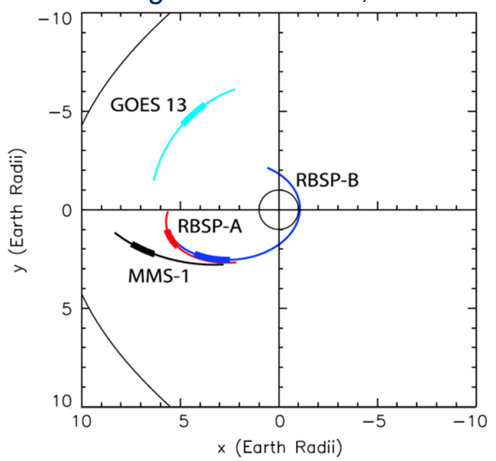

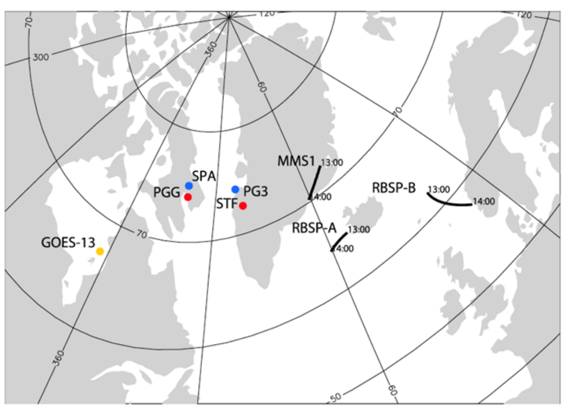

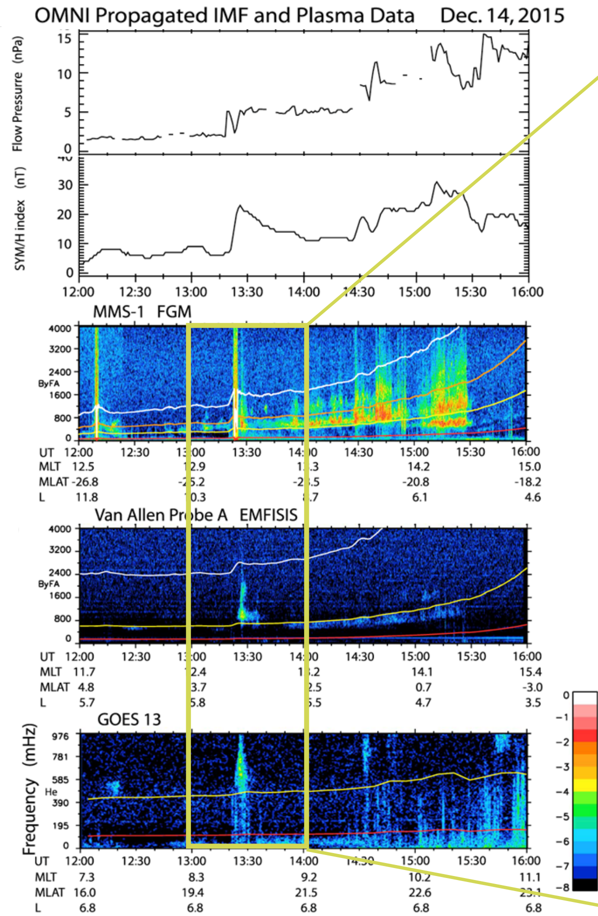

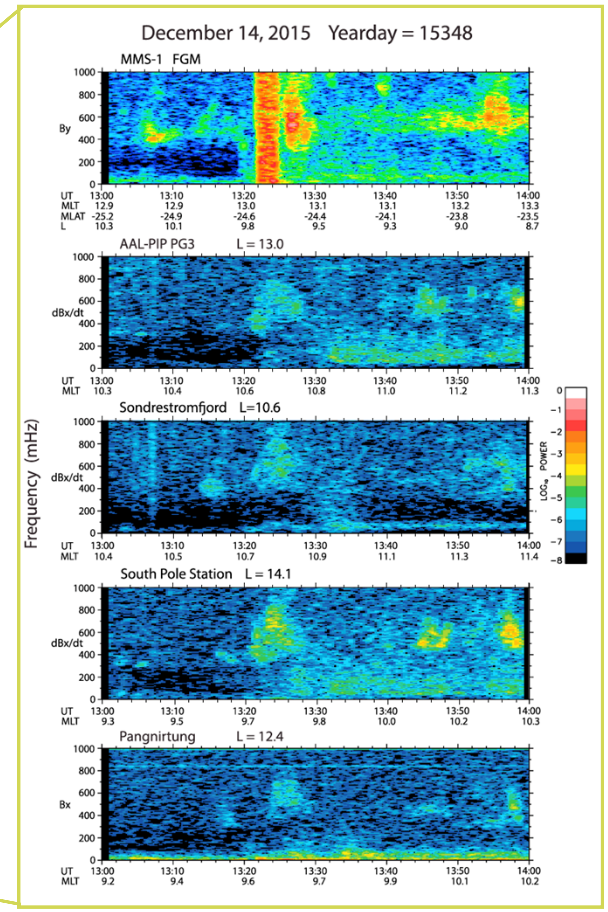

Examples of the extended HSO at work

Timing, causality, and large-scale spatial distribution: Plasmaspheric mass density and refilling

Dent et al., 2006

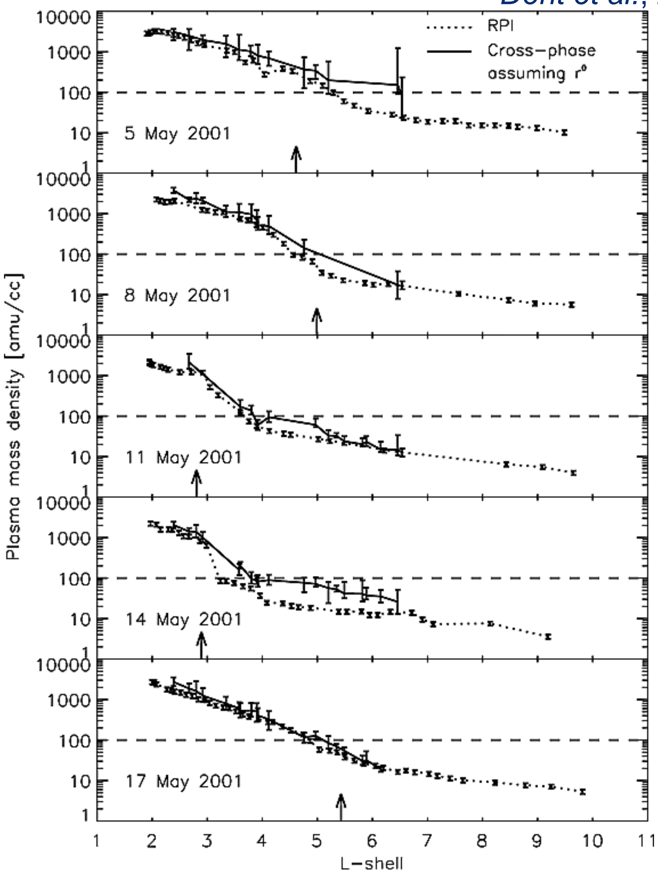

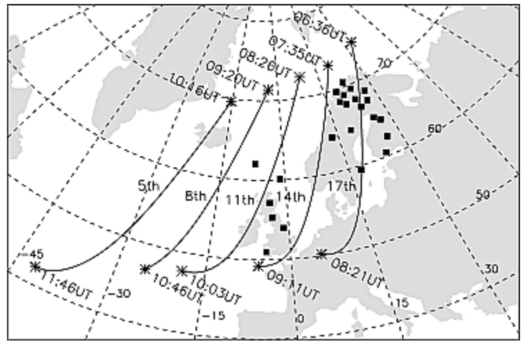

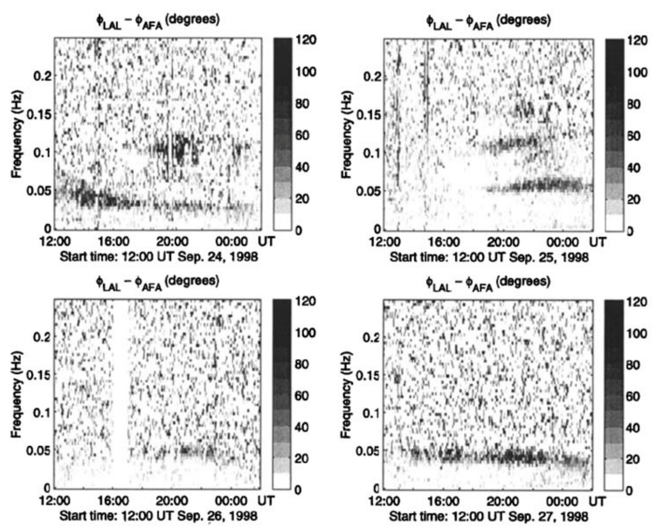

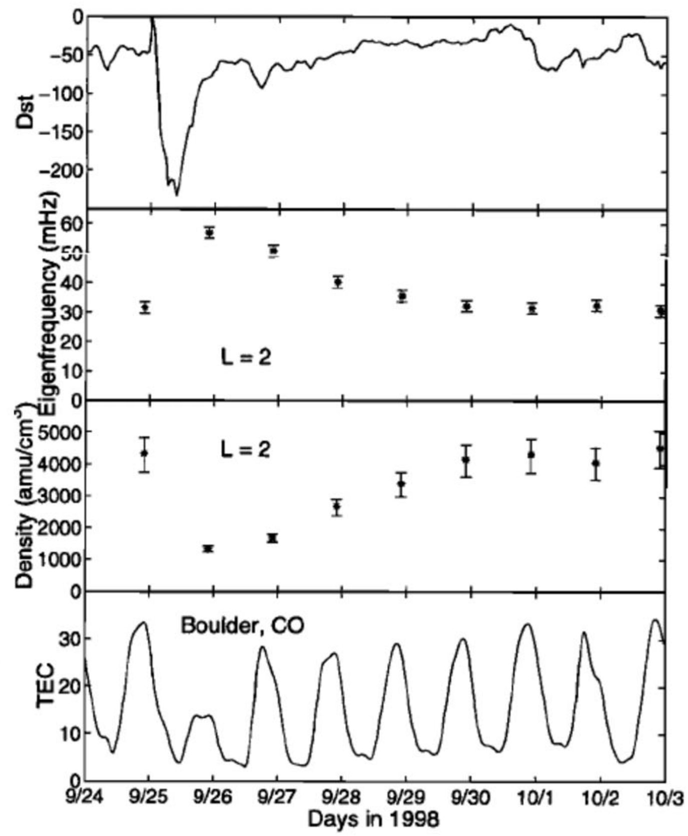

Chi et al., 2002

Things to keep in mind for multi-observatory studies

Caveats and uncertainties

- Understanding timing delays, specifically when comparing upstream solar wind measurements to measurements within the magnetosphere or polar cap region
- Field line and footpoint mapping from spacecraft at large radial distances to the ionosphere and ground, especially for observations in the magnetotail
- Differences in instrument types and capabilities between missions, especially for quantitative comparisons of measurements between different satellite missions

Multi-Point Observations: The Constellation View

Timing and Phase Correlations

Spatial Gradients

Event Reconstruction

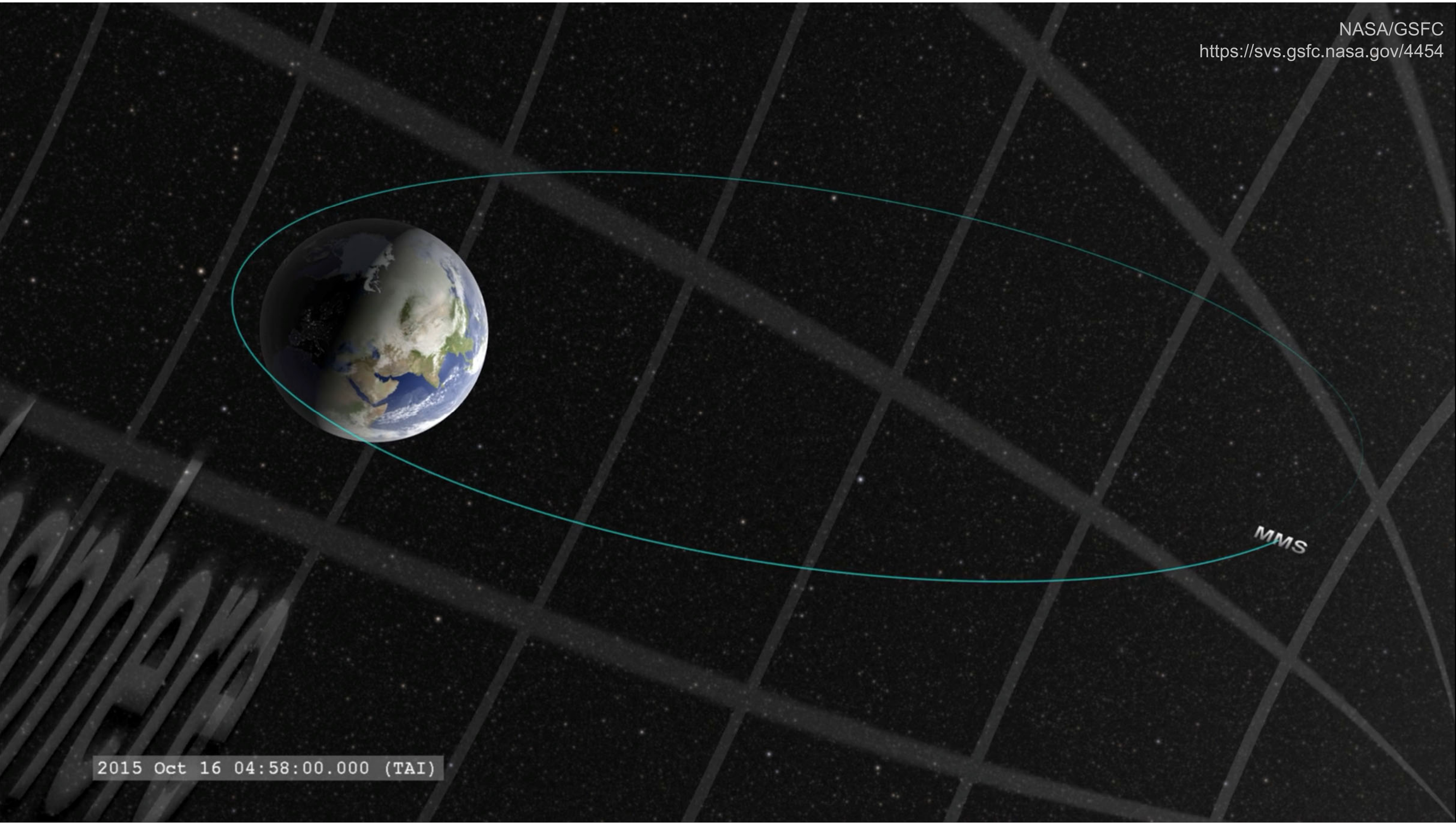
NASA/GSFC
https://svs.gsfc.nasa.gov/4454
MMS
2015 Oct 16 04:58:00.000 (TAI)

Timing Analysis from Constellations

Boundary/Discontinuity Analysis

Haaland et al., 2004

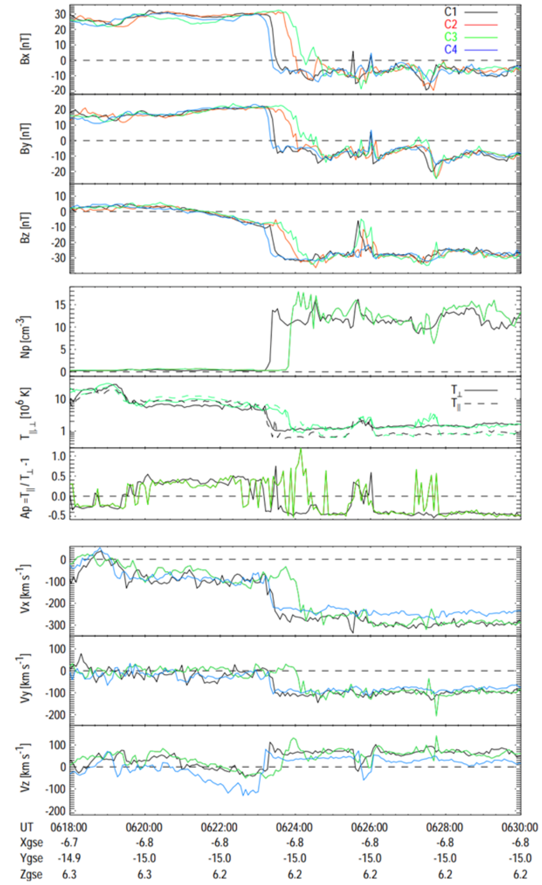

- Discontinuity analysis uses the relative location and time difference between multiple spacecraft to determine the orientation and motion of a structure:

$$(V_{\mathrm{sh}}^{\mathrm{arb}} t_{\alpha\beta}) \cdot \hat{\boldsymbol{n}} = \boldsymbol{r}_{\alpha\beta} \cdot \hat{\boldsymbol{n}} \quad \Longrightarrow \quad \begin{pmatrix} \boldsymbol{r}_{12} \\ \boldsymbol{r}_{13} \\ \boldsymbol{r}_{14} \end{pmatrix} \cdot \frac{1}{V_{\mathrm{sh}}^{\mathrm{arb}}} \begin{pmatrix} n_x \\ n_y \\ n_z \end{pmatrix} = \begin{pmatrix} t_{12} \\ t_{13} \\ t_{14} \end{pmatrix}$$

(*Schwartz*, 1998)

- Generally assumes a planar boundary or structure with a constant velocity, thickness, or acceleration
  - Has been used typically to determine properties of large-scale boundaries like the magnetopause (e.g., *Haaland et al.*, 2004) and the bow shock (e.g., *Russell et al.*, 1983; *Schwartz*, 1998)

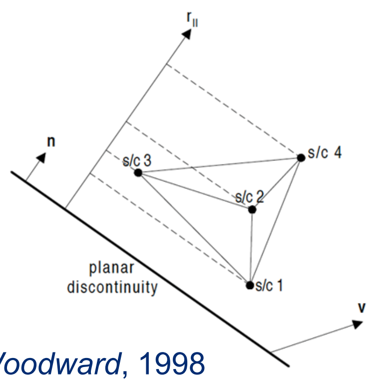

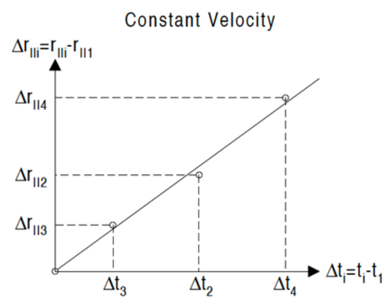

Dunlop & Woodward, 1998

Timing Analysis from Constellations

Phase Differencing

- Using the known separation of individual spacecraft and the assumption that all spacecraft are observing the same waveform, the time difference in the phase of the waveforms between each location can determining the wave vector direction (e.g., *Balikhin et al.*, 1997; *Pinçon & Glassmeier*, 2008)
- Cross-correlation analysis of the waveforms are used to determine a time lag between observing points
- Four four spacecraft, there are multiple triplet-pair combinations which can be used to determine an average wave vector (**k**) and standard deviations in the results (e.g., *Lee et al.,* 2019)

Liu et al., 2017

$$A(\boldsymbol{r}, t) = \sum_{\omega} A_{\omega} \exp i\,(\boldsymbol{k} \cdot \boldsymbol{r} - \omega t) + c.c.$$

$$\begin{aligned} \Delta\psi(\omega) &= \psi_{\alpha}(\omega) - \psi_{\beta}(\omega) \\ &= (\boldsymbol{k} \cdot \boldsymbol{r}_{\alpha} - \omega t) - (\boldsymbol{k} \cdot \boldsymbol{r}_{\beta} - \omega t) \\ &= |\boldsymbol{k}||\boldsymbol{r}_{\alpha\beta}| \cos(\theta_{kr}) \end{aligned}$$

(*Pinçon & Glassmeier*, 2008)

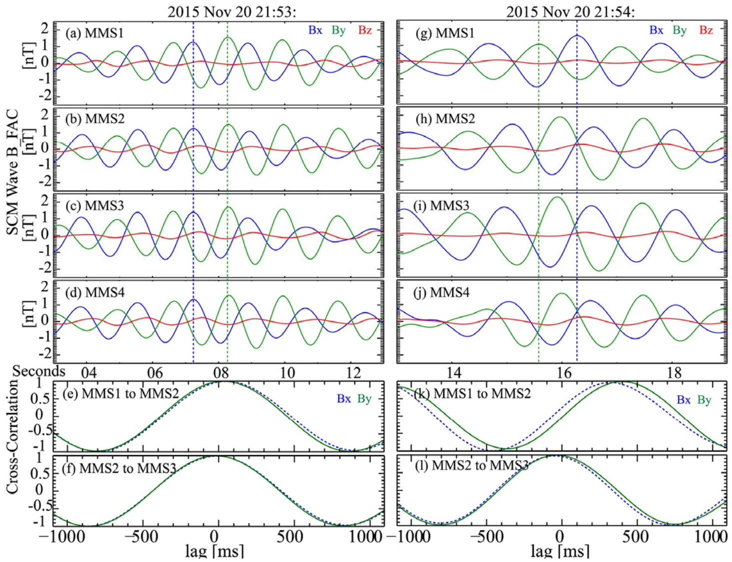

Spatial Analysis from Constellations

Gradients in the Magnetic Field

- Several methods for estimating spatial variations in the magnetic field, extricating current density, and determining properties of magnetic field structures like flux ropes/FTEs
- Applied point-wise in time to disentangle temporal versus spatial changes
- Some examples utilizing the magnetic field gradient, divergence, and curl:
  - Maximum Directional Derivative and Spatiotemporal Differencing methods (e.g., *Shi et al.*, 2005; 2006)
  - Magnetic rotation analysis and magnetic curvature (e.g., *Shen et al.*, 2003; 2007; *Zhao et al.*, 2016; *Akhavan-Tafti et al.*, 2019)
  - **Curlometer (e.g., *Dunlop et al.* 1988; 2002; *Dunlop & Harvey*, 2008; *Robert et al.*, 1998)**

Gradients in the Magnetic Field

The Tetrahedron, Reciprocal Vectors, and the Curlometer

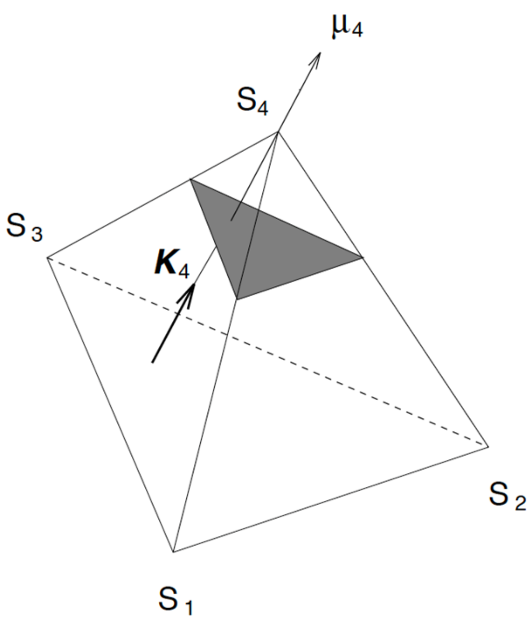

$$k_4 = \frac{r_{12} \times r_{13}}{r_{14}.(r_{12} \times r_{13})}$$

Chanteur et al., 1998

- For 3D linear gradients, a minimum number of 4 spacecraft can be used if the constellation has tetrahedral configuration
  - Three distinct surfaces, with a fourth surface of the tetrahedron available for redundancy
- Deriving gradients using a tetrahedral configuration can be described through the volumetric tensor and reciprocal vectors

(*Chanteur*, 1998; *Harvey*, 1998; *Chanteur & Harvey*, 1998; *Vogt et al.*, 2008)

$$\mathrm{R} = \frac{1}{N}\sum_{\alpha=1}^{N}(\boldsymbol{r}_\alpha - \boldsymbol{r}_b)(\boldsymbol{r}_\alpha - \boldsymbol{r}_b)^T = \frac{1}{N}\sum_{\alpha=1}^{N}\boldsymbol{r}_\alpha\boldsymbol{r}_\alpha^T - \boldsymbol{r}_b\boldsymbol{r}_b^T \; ; \quad \boldsymbol{k}_\alpha = \frac{\boldsymbol{r}_{\beta\gamma} \times \boldsymbol{r}_{\beta\lambda}}{\boldsymbol{r}_{\beta\alpha} \cdot (\boldsymbol{r}_{\beta\gamma} \times \boldsymbol{r}_{\beta\lambda})}$$

$$\nabla g \simeq \nabla \tilde{g} = \sum_{\alpha=0}^{3}\boldsymbol{k}_\alpha g_\alpha \; ; \quad \nabla \cdot \boldsymbol{V} \simeq \nabla \cdot \tilde{\boldsymbol{V}} = \sum_{\alpha=0}^{3}\boldsymbol{k}_\alpha \cdot \boldsymbol{V}_\alpha \; ; \quad \nabla \times \boldsymbol{V} \simeq \nabla \times \tilde{\boldsymbol{V}} = \sum_{\alpha=0}^{3}\boldsymbol{k}_\alpha \times \boldsymbol{V}_\alpha$$

- The assumption of linear gradients and the use of reciprocal vectors forms the basis of the curlometer technique: a four-point magnetic field measurement to evaluate the integral form of Ampere's law

$$\mu_0 < \boldsymbol{J} > (\Delta r_i \Delta R_j) = \Delta B_i \times \Delta R_j - \Delta B_j \times \Delta R_i,$$

(*Dunlop et al.*, 2016)

$$\text{e.g., } \mu_0 < \boldsymbol{J} >_{123} (\Delta r_{12} \Delta R_{13}) = \Delta B_{12} \cdot \Delta R_{13} - \Delta B_{13} \times \Delta R_{12}$$

- This provides the average current density vector at the barycenter of the constellation

Gradients in the Magnetic Field

The Tetrahedron, Reciprocal Vectors, and the Curlometer

- The curlometer has been widely used to calculate the current density of various structures throughout the magnetosphere, in the magnetosheath, and in the solar wind using Cluster and MMS

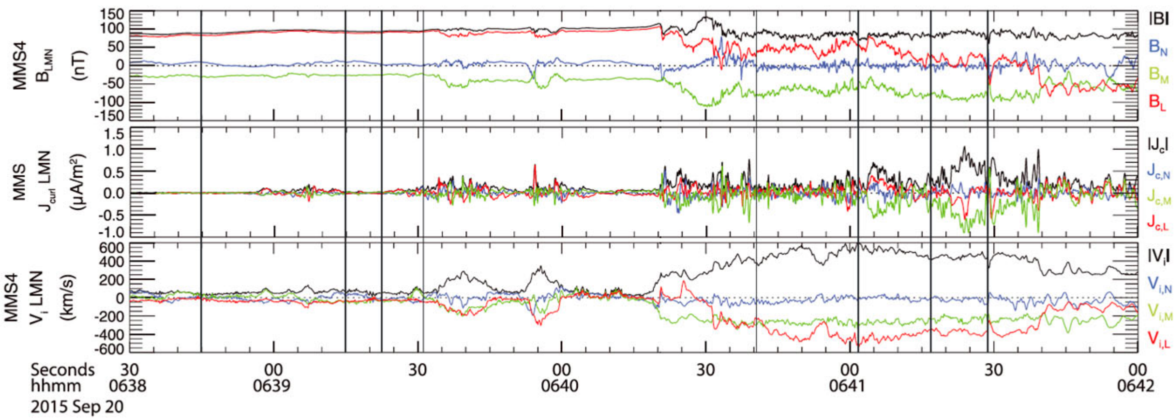

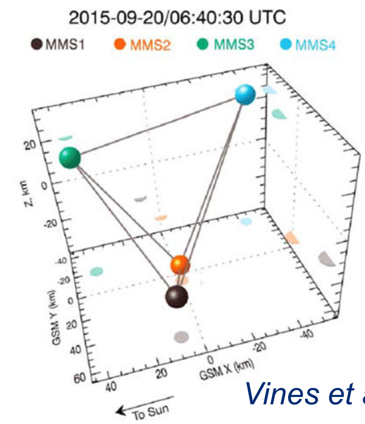

Vines et al., 2017

- The separations and configuration of the constellation limits the scale sizes and dimensionality of the current densities that can be obtained (i.e., where the linear gradient approximation is valid)
- A metric of "goodness" of curlometer results comes from $|\nabla\cdot\mathbf{B}|/|\nabla\times\mathbf{B}|$
  - Since $\nabla\cdot\mathbf{B}$ should ideally be 0, this ratio should be very small
- Another metric of goodness is the tetrahedral quality factor, *Q*, derived from the volume of the tetrahedron
  - For an ideal tetrahedron with MMS, $Q = 1$ (i.e., the "Q_{RR} parameter" in *Robert et al.*, 1998b)

Gradients in the Magnetic Field

Working with Other Configurations

- Curlometer and gradient-based approaches have been used with other constellations having less than 4 satellites and/or in an irregular/non-tetrahedral configuration (e.g., *Dunlop et al.*, 2015; 2020; *Shen et al.*, 2012a,b; *Yang et al.*, 2016; *Artemyev et al.*, 2019)

- The less spacecraft, the more assumptions:
  - time stationarity of gradients or structure
  - direction and structure of the magnetic field and current density (i.e., force-free **B** or magnetic field-aligned **J**)
  - measure of only 1 or 2D current densities

Pseudo-tetrahedron:

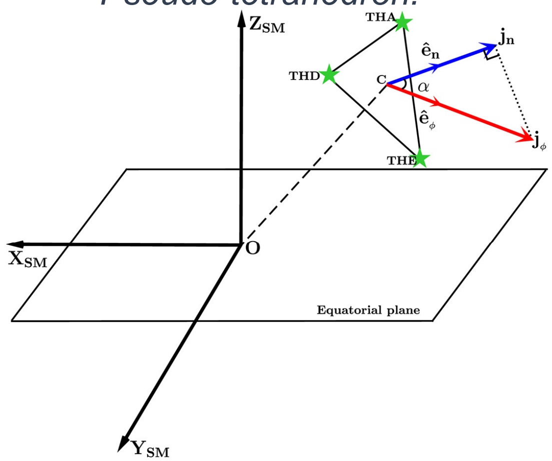

Yang et al., 2016

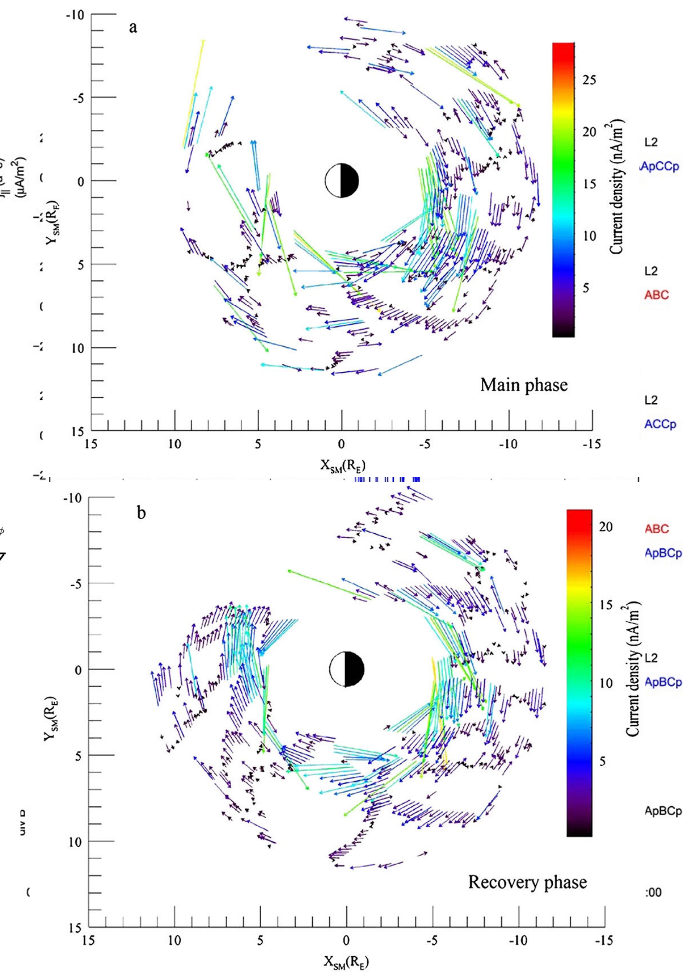

Gradients in the Magnetic Field

Making Use of Mega-constellations and Networks: The AMPERE dataset

- Collect all horizontal δB observations in a 10-minute window from 66 Iridium satellites
  - Assumption of radial currents only, and so only a toroidal perturbation magnetic field
- Fit to a regular grid through spherical cap harmonic expansion
  - Linear interpolation to estimate the δB values between tracks
- In solving the system to obtain FACs, the squared difference between the data and the estimated values from the SCHA basis functions are minimized using Singular Value Decomposition (SVD)

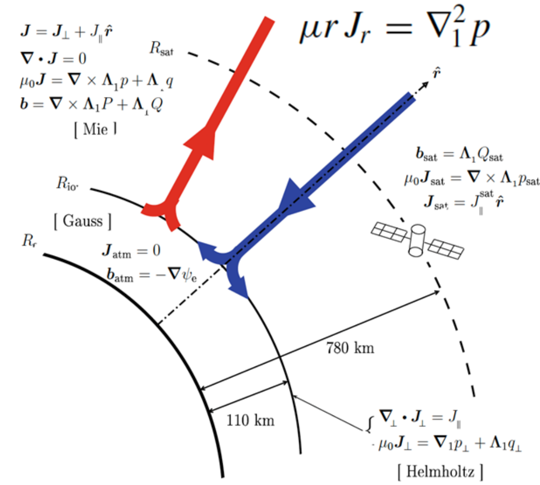

Green et al., 2006; *Waters et al.*, 2020

2015-06-22
19:40 UT
Northern Hemisphere

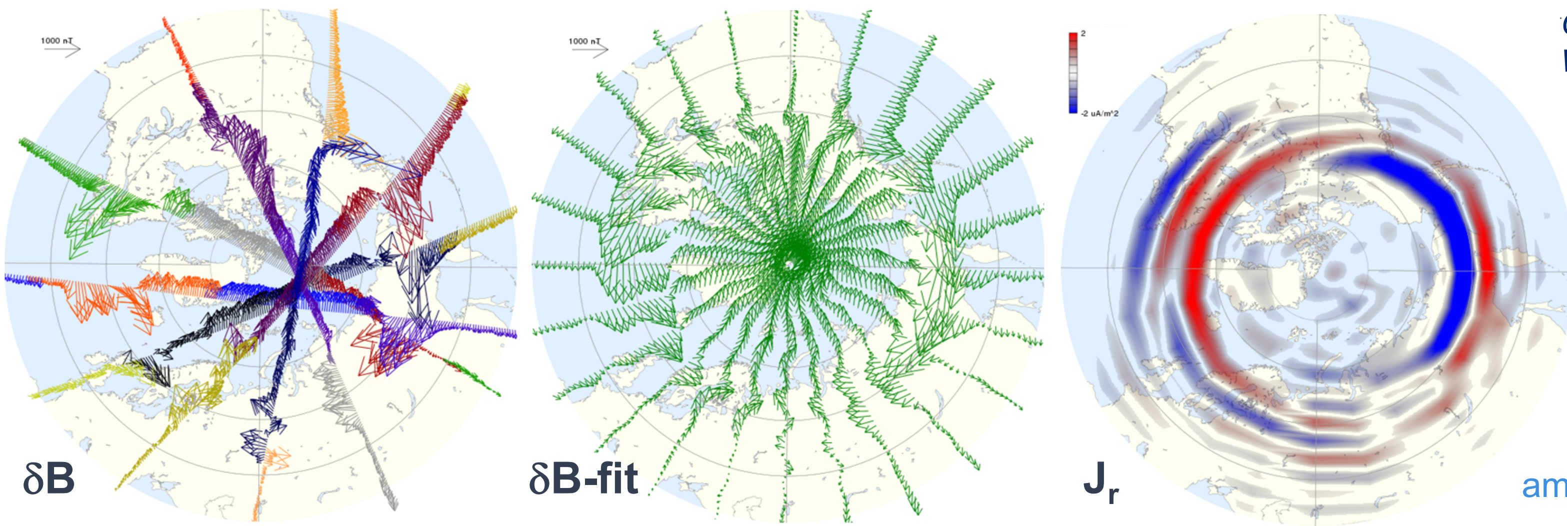

ampere.jhuapl.edu

Gradients in the Plasma

Application to the Generalized Ohm's Law

- Extension of the classic Ohm's law relating current density, electric field, and conductivity:

$$\mathbf{E}+\mathbf{U}_e\times\mathbf{B}=\eta\mathbf{J}-\frac{1}{en}\nabla\cdot\overleftrightarrow{\mathbf{P}}_e+\frac{m_e}{en}\left(\frac{\partial\mathbf{J}}{e\partial t}+\nabla\cdot n(\mathbf{U}_i\mathbf{U}_i-\mathbf{U}_e\mathbf{U}_e)\right)$$

Torbert et al., 2016; *Hesse et al.*, 2014

- Using assumptions of linear gradients of the fields and plasma between the individual spacecraft, divergence of electron pressure and inertial terms are calculated
- For studies of magnetic reconnection, each term of the generalized form is evaluated to better understand what is contributing to energy conversion

Genestreti et al., 2018

Torbert et al., 2016

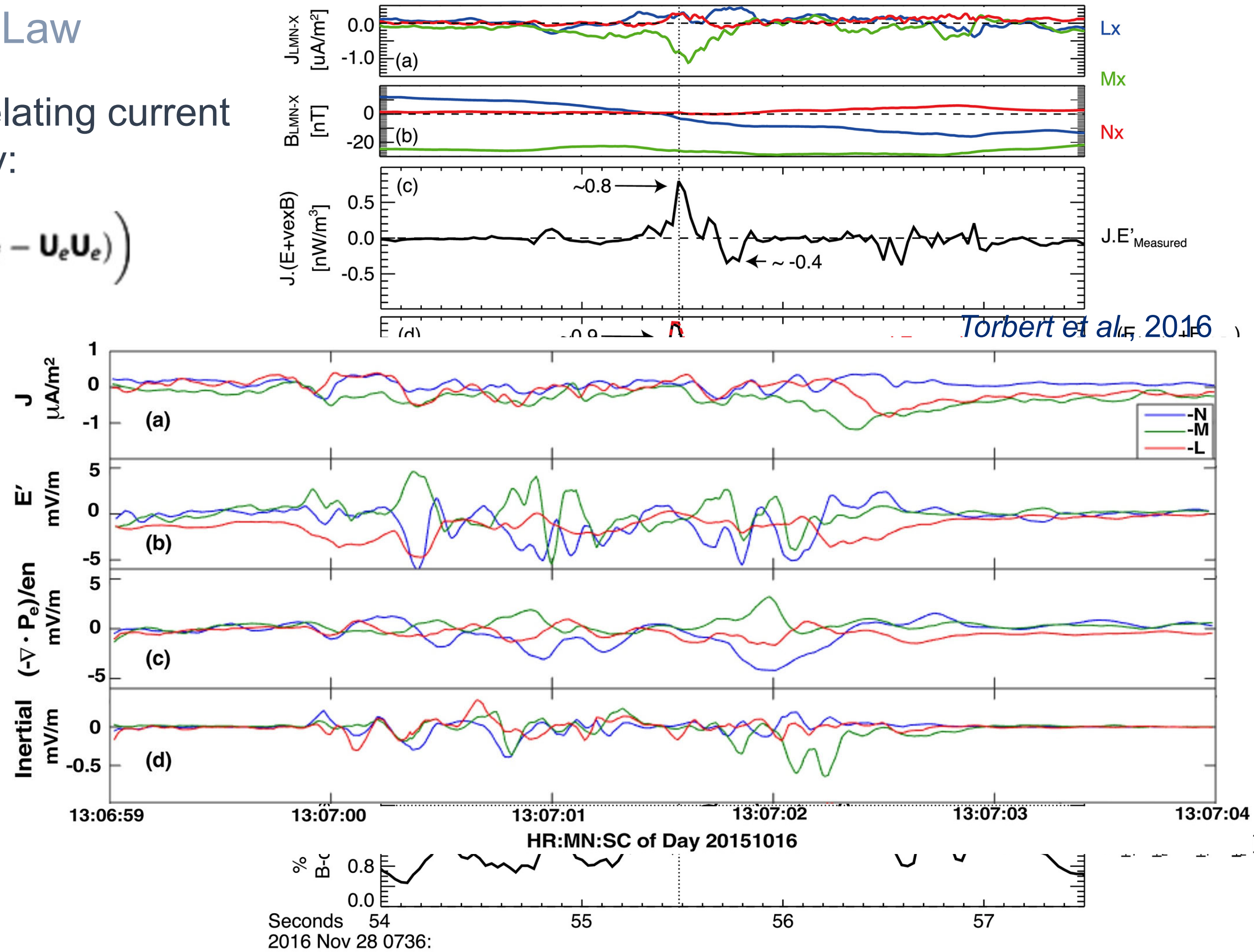

Reconstructions from Constellation Data

Grad-Shafranov Reconstruction

- Assuming structures are 2D and magnetohydrostatic (i.e., time independent and negligible inertial effects) in the frame of the moving structure (e.g., *Sonnerup et al.*, 2008)
- Solves the Grad-Shafranov equation describing force balance for this 2D structure:

$$\frac{\partial^2 A}{\partial x^2} + \frac{\partial^2 A}{\partial y^2} = -\mu_0 \frac{dP_t}{dA} = -\mu_0 j_z(A),$$

  - Observations of the magnetic field and isotropic plasma pressure are used as initial values
- Initially developed for single-spacecraft measurements (e.g., *Sonnerup & Guo*, 1996; *Teh et al.*, 2011) and then extended to multi-point observations (e.g., *Hasegawa et al.*, 2005; 2007)
  - The multi-point method merges individual field and potential maps from each spacecraft
  - Individual maps used to constrain the invariant axis orientation

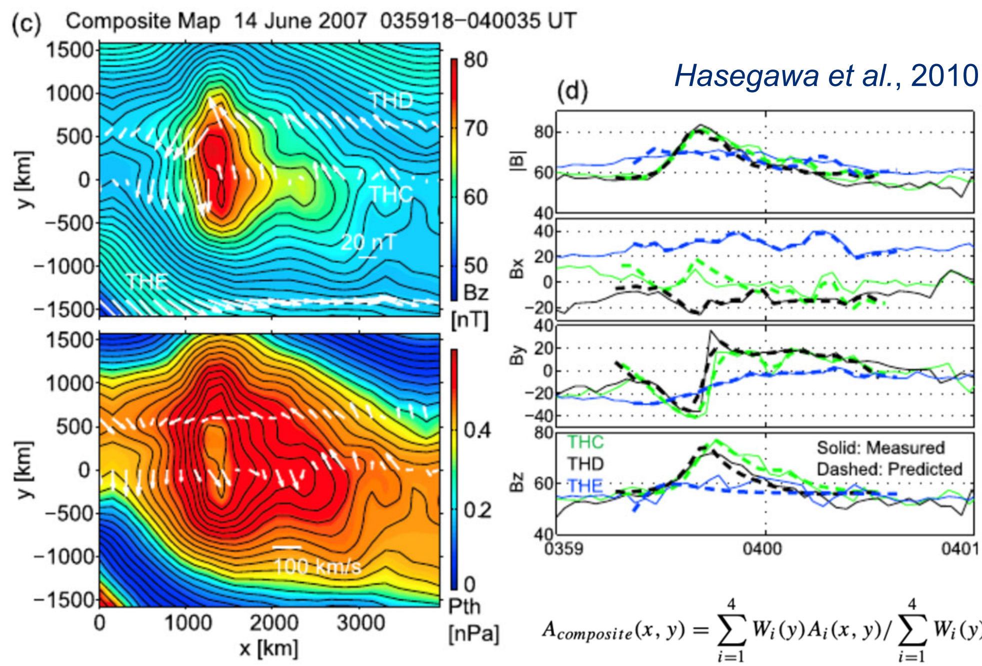

Hasegawa et al., 2010

$$A_{composite}(x, y) = \sum_{i=1}^{4} W_i(y) A_i(x, y) / \sum_{i=1}^{4} W_i(y),$$

Reconstructions from Constellation Data

MHD-based Reconstruction

- Uses multi-point observations as initial inputs for MHD descriptions of steady, 2D magnetic and velocity fields
  - Solving the various forms of Ohm's law under different assumptions of plasma behavior (i.e., satisfying the frozen-in condition or allowing for different effects when that condition is violated)
- Depending on the structure or region of interest, and on the available observations, multiple forms of this type of reconstruction have been developed:
  - Ideal MHD (*Sonnerup et al.*, 2008; *Teh et al.*, 2009)
  - Hall and resistive MHD (*Teh et al.,* 2010; *Sonnerup & Teh*, 2009)
  - Electron MHD (EMHD) (*Sonnerup et al.*, 2016; *Hasegawa et al.*, 2017; 2018)

Hasegawa et al., 2017

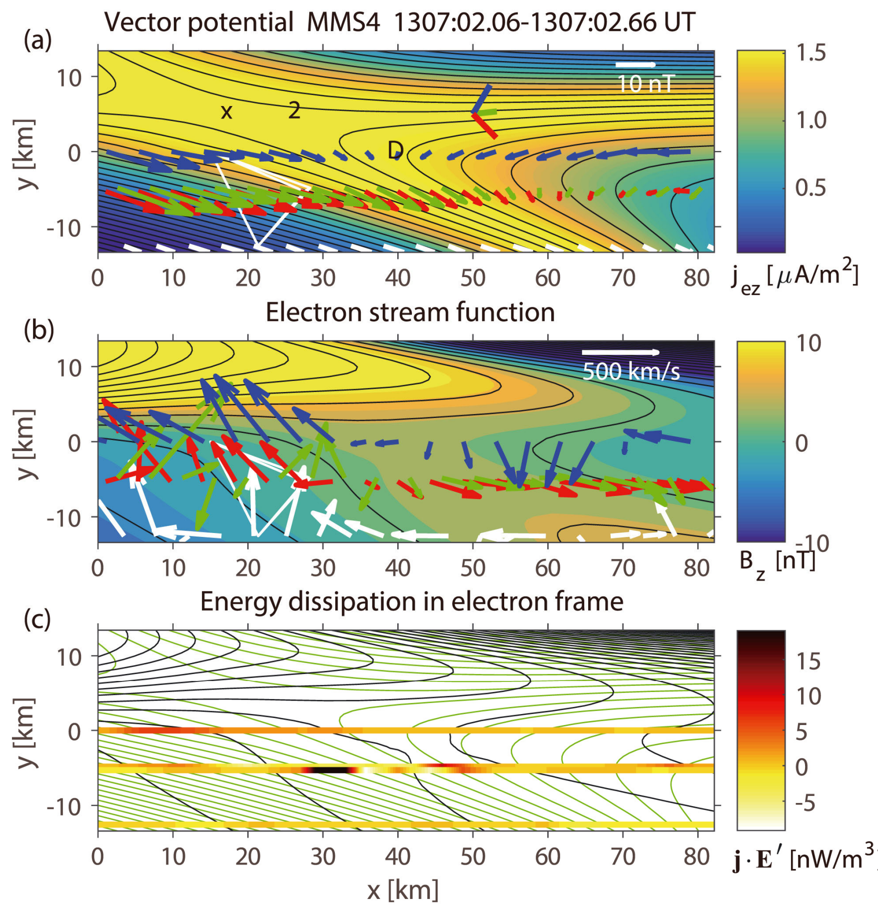

Reconstructions from Constellation Data

Polynomial Expansion Reconstruction

- Quadratic expansion of the magnetic field and current density measured at the 4 MMS spacecraft, with the constraint ∇·**B** = 0
  - Because of the ability to measure plasma moments to high fidelity, **J** from each spacecraft can be used

$$B_j = B_{0j} + \sum_k x_k \left(\partial_k B_j\right)_0 + \S \sum_{k,l} x_k\, x_l \left(\partial_k \partial_l B_j\right)_0$$

Torbert et al., 2020

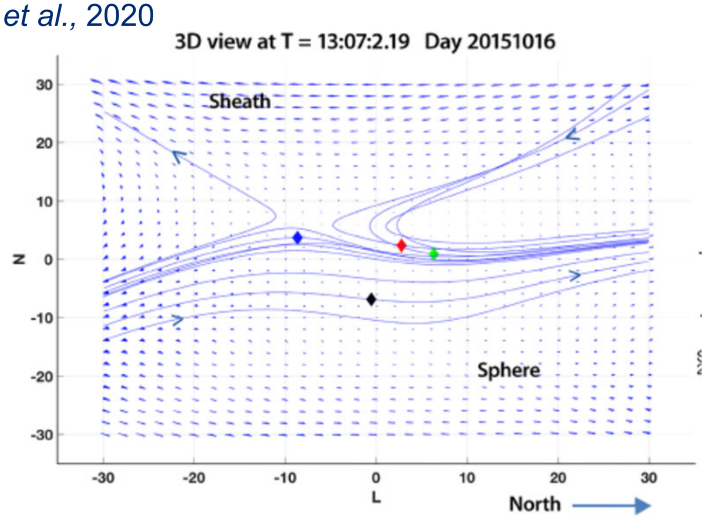

- Expansions of varying complexity, from linear to fully 3D quadratic formulation with additions of cubic terms, and the use of least squares fits to the measurements are explored in *Denton et al.* 2020

3D Reduced Quadratic Model

Denton et al., 2020

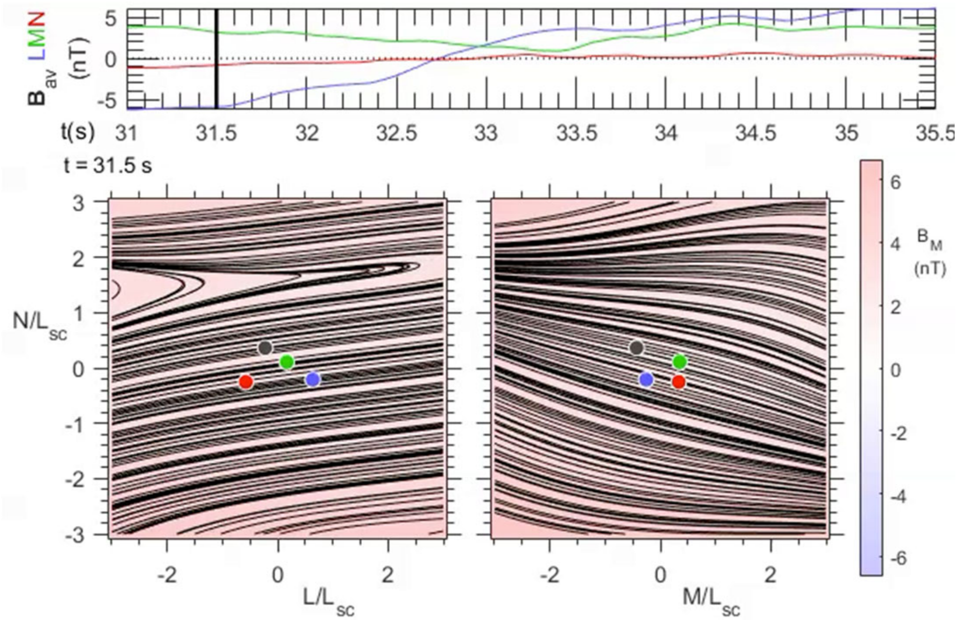

Multi-Point Observations for our Present and Future

Multi-mission/observatory considerations

- Multi-mission and multi-observatory are incredibly useful for understanding cross-scale dynamics and coupling, and the more datasets we have, the more kinds of conjunctions we can consider in trying to understand larger-scale processes and responses of the magnetosphere
- As missions are extended and future missions are implemented, continue to increase collaboration between active missions and observatories, such as conducting campaign events and planning of opportune conjunctions
- Consider how to better incorporate remote sensing techniques in magnetospheric research, whether from satellites or ground-based observations, particularly for system-wide contextual observations

Satellite constellation considerations

- Coupled with the increasing number of satellite missions and ground-based observatories, ever-larger constellations are on their way, especially with the advances in CubeSat/SmallSat capabilities and launch vehicle infrastructure
- As we think about constellations, recognize the value of copious good enough measurements versus just a few exquisite measurements
- Continue to push forward in how we process, analyze, and visualize all of the data streams from individual satellites/observatories, including reconstruction techniques and data mining and assimilation

With multi-point measurements and techniques, we can explore system-wide dynamics and local variations beyond what can be done with just one observatory.

Using multi-point techniques: Where to start?

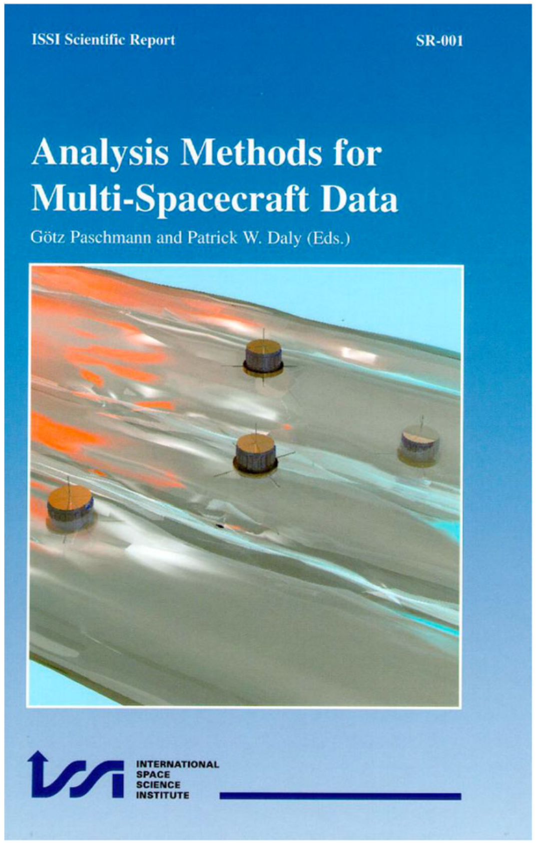

1998, 2000

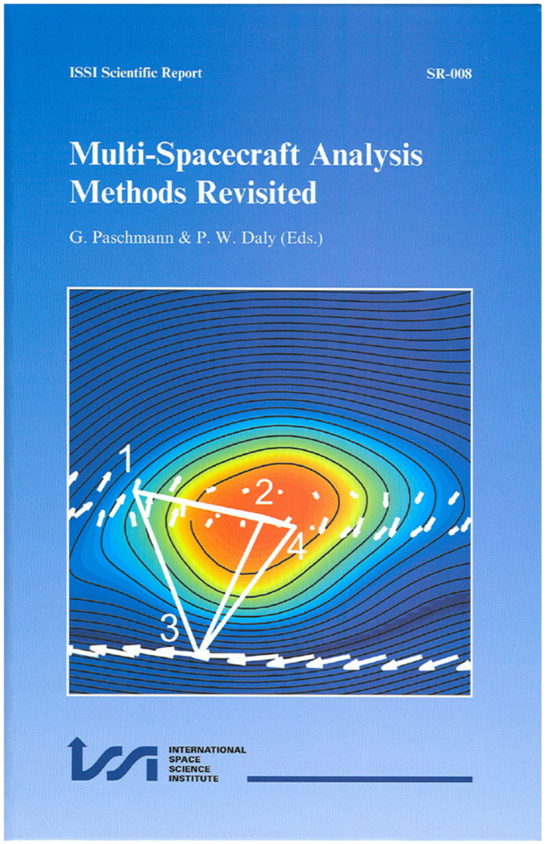

2008

2020

JOHNS HOPKINS
APPLIED PHYSICS LABORATORY

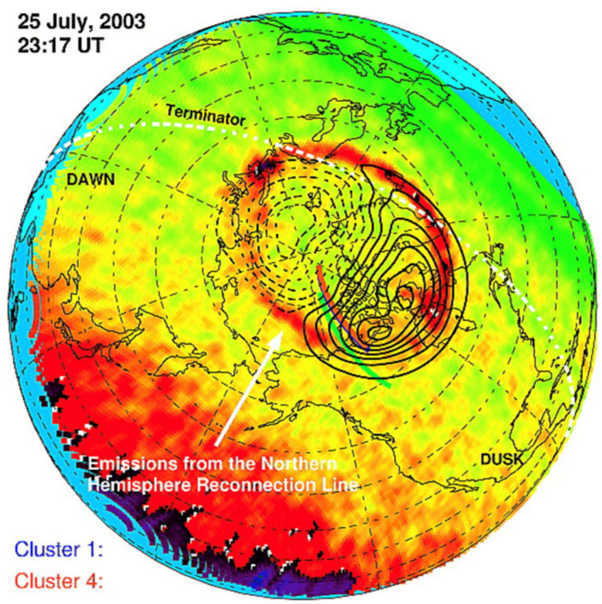

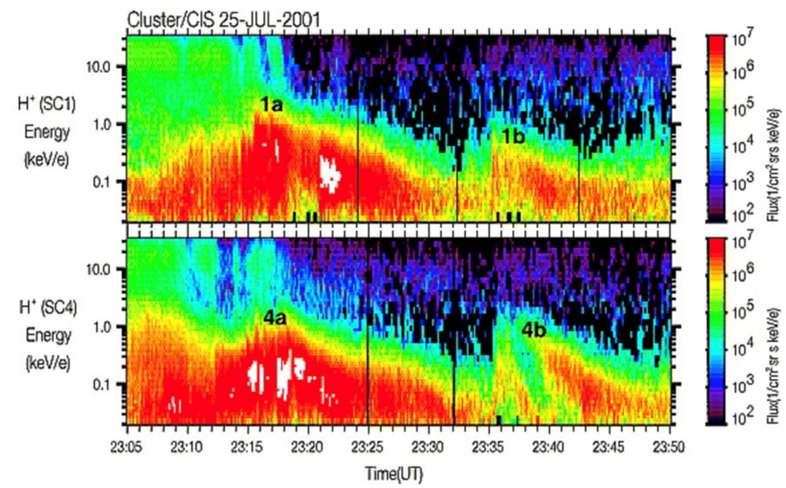

Trattner et al., 2001